Electronic Materials Letters, Vol. 1, No. 2 (2005), pp. 121-126

Realization of *p*-Type ZnO Using Zn_3As_2 and Zn_3P_2 as Doping Source Materials

Veeramuthu Vaithianathan, Sang Sub Kim*, and Byung-Teak Lee

Department of Materials Science and Engineering, Chonnam National University, Gwangju 500-757, Korea

A report on the preparation of arsenic-, and phosphorus-doped *p*-type ZnO films is presented, which involves As and P incorporation during pulsed laser deposition using Zn_3As_2 and Zn_3P_2 as the doping source materials, respectively. The room temperature Hall measurements reveal that the *n*-type arsenic-, and phosphorus-doped as-grown ZnO films show *p*-type behavior after being thermally annealed at 200 °C, and at temperatures between 600 °C and 800 °C, respectively. This indicates that only a proper thermal annealing treatment favors *p*-type conversion. A photoluminescence emission associated with the acceptors is observed only in the *p*-type ZnO films; it was not present in the films showing the *n*-type behavior. X-ray absorption near-edge structure measurements reveal both As and P occupy O in the ZnO lattice, meaning that As_O and P_O are the acceptors in the arsenic-, and phosphorus-doped, *p*-type ZnO films. Our results suggest that Zn_3As_2 and Zn_3P_2 are promising *p*-type doping source materials for use in preparing reliable *p*-ZnO.

Keywords: ZnO, pulsed laser deposition, doping, photoluminescence

1. INTRODUCTION

In the field of optoelectronic devices that work in both the ultra violet and blue regions, several trends have been leading the demand for research on the subject of new materials. Towards this end, in recent years ZnO appears to have become the semiconducting material of choice, and it has been attracting a good deal of attention. It is seen as a highly preferable material for use in not only optoelectronic devices[1,2], but also in short wavelength lasers in optical memory[3], solar cells[4], sensors[5], and surface acoustic wave devices[6]. ZnO reveals excellent characteristics, such as large exciton binding energy (60 meV), a direct bandgap of 3.37 eV, and the possibility of modifying the band gap toward lower and higher energies by alloying it with CdO and MgO, respectively. To facilitate further progress, there is a need for the development of a process allowing the growth of high quality ZnO films with high doping densities (particularly, *p*-type).

Although *n*-ZnO can easily be fabricated with high carrier concentrations and other desired properties, the growth of this material with *p*-type doping has proven to be very difficult mainly due to a self-compensation mechanism involving native point defects such as oxygen vacancies (V_o) or zinc interstitials (Zn_i)[7]. Many researchers have recently demonstrated that the group V elements such as N[8-16], P[17-22], As[23-29] are potential candidates that produce a shallow acceptor level in ZnO. Apart from these *p*-type dopants, Sb [30] and Cu[31] have also been proposed for making *p*-type ZnO. In addition, a codoping process was proposed to prepare *p*-type ZnO[32]. However, unfortunately, obtaining reliability in *p*-type ZnO films is still difficult, and also a lack of consistency has been observed in the conductivity of ZnO films while using the same *p*-type source material[17,18]. Thus, it seems important to investigate the behavior of a doping issue with suitable *p*-type source materials. Moreover, the mechanism that governs the dopant behavior is also not clear yet, indicating that p-type doping in ZnO still remains a recognized problem.

In order to seek better *p*-type source materials, in the present study we used Zn_3As_2 and Zn_3P_2 as the doping source materials, respectively, for As and P to grow *p*-type ZnO with the use of the pulsed laser deposition (PLD) technique.

2. EXPERIMENTAL DETAILS

For the present work, undoped, As-doped, and P-doped ZnO films were grown on Al_2O_3 (0001) substrates utilizing the PLD technique. During all the experiments, the substrate temperature and the O_2 pressure were kept at 600 °C and 5×10^{-2} Torr, respectively. The As-, and P-doped ZnO targets

*Corresponding author: sangsub@chonnam.ac.kr

were prepared by a conventional ceramic powder process by mixing, respectively, Zn_3As_2 and Zn_3P_2 with ZnO. Before being attached into the substrate holder, the Al_2O_3 substrates were cleaned successively with trichloroethylene, acetone and ethanol in an ultrasonic bath. The growth chamber was pumped down to a base pressure of 5×10^{-6} Torr prior to its being back filled with an O_2 ambient. We used a pulsed KrF excimer laser (248 nm, 30 ns duration) at a repetition rate of 7 Hz to ablate the targets. The laser beam energy was typically set at 30 mJ/pulse.

Rapid thermal annealing (RTA) treatment was carried out in a flowing N_2/O_2 ambient at a pressure of 1 atm at various temperatures. The film crystallinity and growth orientation were examined by X-ray diffraction (XRD). Atomic force microscopy (AFM) was used to observe the microstructure of the films. The electrical properties of both the as-grown and annealed films were investigated by using the four-point van der Pauw Hall measuring configuration at room temperature. To study the optical properties of the films, room as well as low temperature photoluminescence (PL) measurements were performed using a He-Cd laser with a wavelength of 325 nm. The X-ray absorption near-edge structure (XANES) technique was used to investigate the electronic structure around the dopant in the As-, and P-doped ZnO films.

3. RESULTS AND DISCUSSION

3.1. As doping in ZnO using Zn_3As_2

The ZnO films containing 1 mol% As ($ZnO:As_{0.01}$) were deposited by PLD. In order to obtain reliable results, we evaluated the structural, microstructure and optical properties for several $ZnO:As_{0.01}$ films. A typical XRD pattern of the $ZnO:As_{0.01}$ films is presented in Fig. 1(a). As shown, the film exhibits only the peaks that correspond to the ZnO (0002) and (0004) plane along with the Al_2O_3 (0006) substrate reflection, indicating that the films grew with the preferred c-axis orientation and also with the single phase of ZnO. In order to investigate the epitaxial nature of the films, x-ray pole figure measurements for the ZnO {101} reflections were conducted and the typical result is shown in the inset of Fig. 1(a). The x-ray pole figure reveals a 60° space separation between the peaks, suggesting that the $ZnO:As_{0.01}$ films were well aligned with the substrate in both the in-plane and out-of-plane direction. As shown in Fig. 1(b), the typical AFM image taken from the $ZnO:As_{0.01}$ films reveals a smooth surface, with the root mean square (RMS) roughness of ~0.44 nm. At room temperature, the typical PL spectrum of the $ZnO:As_{0.01}$ films (see Fig. 1(c)) shows only an intense near band edge emission at 3.28 eV, showing their high optical quality.

The Hall measurements were conducted at room temperature and typical results are presented in Table. 1[29]. The

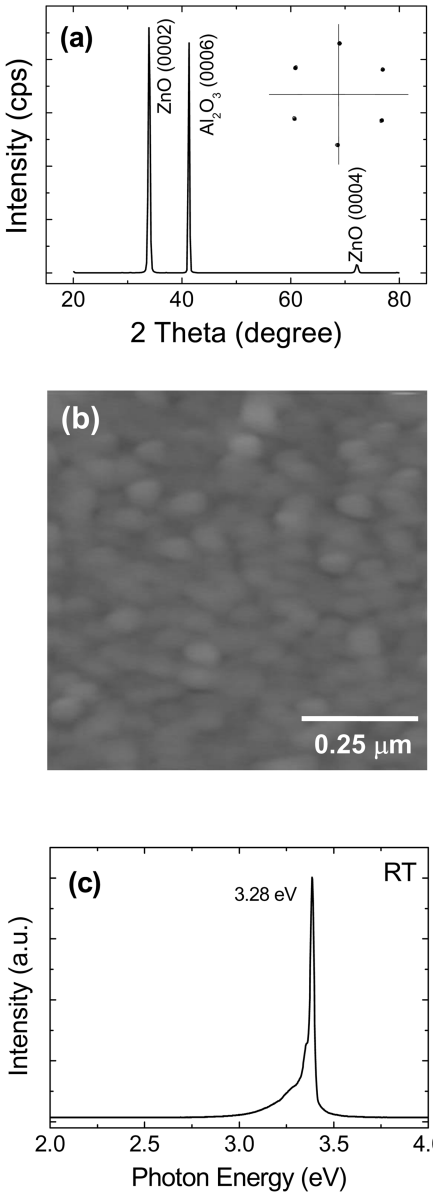

Fig. 1. (a) Typical θ-2θ XRD pattern of the $ZnO:As_{0.01}$ films, showing only the peaks corresponding to the (0002) and (0004) reflections, (b) Typical AFM image of the $ZnO:As_{0.01}$ films exhibiting a smooth surface with the root mean square roughness of ~0.44 nm, and (c) Typical RT PL spectrum of the $ZnO:As_{0.01}$ films revealing only a strong near band edge emission at 3.28 eV. Note that no defect level peaks around 2.2 eV can be observed in the PL spectrum, revealing their optimal optical quality.

$ZnO:As_{0.01}$ films exhibit *n*-type conductivity in the as-grown state, like that of the undoped ZnO films. After RTA, the Hall effect measurements reveal considerable changes in the electrical behavior and optical property of the $ZnO:As_{0.01}$ films. The conductivity of the as-grown $ZnO:As_{0.01}$ films was changed from *n*-type to *p*-type after being annealed at an RTA temperature of 200°C in an N_2 ambient for 2 min. The

Table 1. The typical electrical properties of the undoped ZnO, *n*-type and *p*-type ZnO:$As_{0.01}$ films. The As-doped ZnO films revealed *p*-type conductivity after being annealed at 200°C in N_2 ambient for 2 min.

Samples	Carrier Concentration (cm^{-3})	Mobility (cm^2/V-s)	Resistivity (Ω-cm)
n-type undoped ZnO	1.33×10^{17}	5.05	9.27
n-type As-doped ZnO	2.4×10^{16}	1.32	193
p-type As-doped ZnO	2.48×10^{17} - 1.18×10^{18}	0.83 - 11.4	2.2 - 6.7

hole concentration, mobility and resistivity of the As-doped *p*-type ZnO films are in the range of 2.48×10^{17}–1.18×10^{18} cm^{-3}, 0.83–11.4 cm^2/V-s and 2.2-6.7 Ω-cm, respectively. The typical low temperature (15 K) PL spectrum taken from the As-doped *p*-type ZnO films is shown in Fig. 2. The PL emission observed at 3.354 eV is attributed to the emission bound to the As acceptors, i.e., neutral-acceptor bound exciton (A^o,*X*) emission, while the emission due to A-exciton peak appears at 3.387 eV. We believe that the weak intensity of A^o,*X* emission is indicative of a low As incorporation in the film. It is worth mentioning that the peak around 3.35 eV has been identified as the A^o,*X* emission in the *p*-type ZnO[17,26,28].

Investigation on the chemical environment of the acceptors in *p*-type ZnO will be of importance, and there are three reasons for this. The first has to do with the fact that a recent theoretical work[33] proposed that As at a Zn site (rather than at an O site) would be an acceptor in *p*-type ZnO. This is controversial because the general consensus is that the V group elements such as N, P and As would replace O sites, forming acceptor levels. The second reason comes in light of a study by D.C. Look *et al.*[28], who recently suggested two

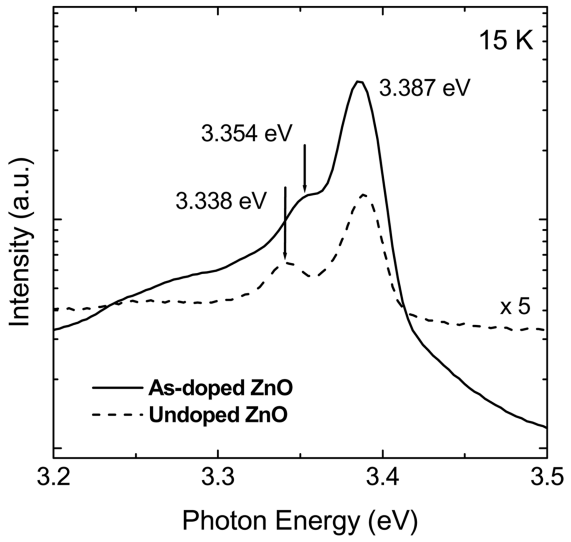

Fig. 2. The typical low temperature (15 K) PL spectra taken from the undoped ZnO film and the *p*-type ZnO:$As_{0.01}$ film. The peak observed at 3.354 eV in the *p*-type ZnO:$As_{0.01}$ film can be attributed to the A^o,*X* emission.

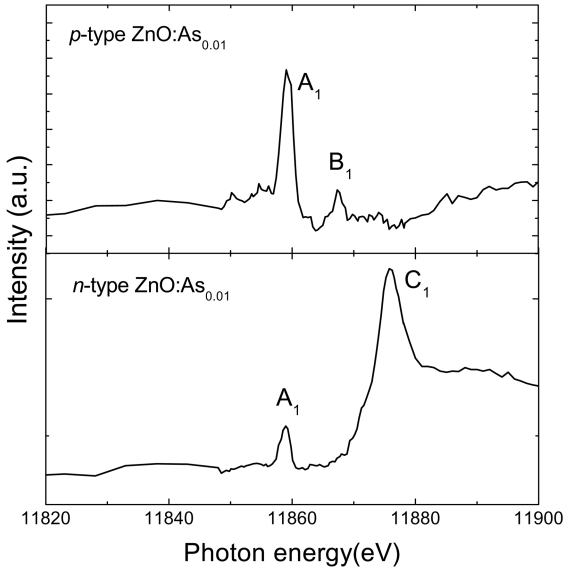

Fig. 3. The As *K*-edge XANES spectra of the *n*-type and the *p*-type ZnO:$As_{0.01}$ films. The spectral features are marked as A_1, B_1 and C_1, representing the different oxidation states of As in the films: As^{3-}, As^0, and As^{5+} respectively.

competing mechanisms involving As acceptor in the As-doped, *p*-type ZnO, namely, either AsO or As_{Zn}-$2V_{Zn}$. Finally, in the case of P-doped *p*-type ZnO films, a rather ambiguous mechanism has been reported[17,18,21]. X-ray absorption near-edge structure (XANES) technique is a versatile tool to study the electronic structure around the dopants in the material[34]. To distinguish the electronic structures between the *n*-, and *p*-type ZnO:$As_{0.01}$ films, XANES spectra were measured using the facilities of the Pohang Accelerator Laboratory (PAL). Figure 3 shows the normalized As *K*-edge XANES spectra of both the *n*-, and *p*-type ZnO:$As_{0.01}$ films. As shown, the *n*-type ZnO:$As_{0.01}$ film reveals two features, namely, A_1 and C_1, which are related to the valance states of As^{3-} and As^{5+}, respectively. The high intensity feature C_1 represents that As primarily occupies the Zn site, forming a As_2O_5 compound, and thereby producing more donors than that of the undoped films. The presence of a small intense A_1 feature suggests that As also generates a smaller number of acceptors (holes) by occupying O sites in the as-grown state. As can be seen, for *p*-type ZnO:$As_{0.01}$ films, the intensity of the feature A_1 sharply increases, and the feature C_1 is no longer seen after RTA. However, a new feature (B_1) corresponding to As^0 arises. The absence of the feature C_1 and an increase in the intensity of the feature A_1 in *p*-type ZnO:$As_{0.01}$ films indicate that As occupies O sites with the valence state of As^{3-}, generating a sufficient number of holes. The results of the XANES measurements strongly suggest that As_O is the acceptor responsible for the *p*-type behavior in the As-doped ZnO films.

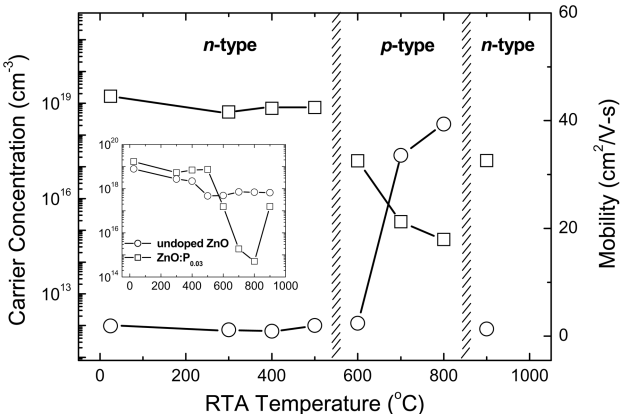

Fig. 4. The effect of the annealing temperature on the carrier concentration and on the mobility of the ZnO:$P_{0.03}$ films. A considerable reduction in the carrier concentration can be observed in the annealing temperature between 600 °C and 800 °C where the ZnO:$P_{0.03}$ films exhibit *p*-type behavior. A comparison between the carrier concentrations of the undoped and the ZnO:$P_{0.03}$ films is shown in the inset figure.

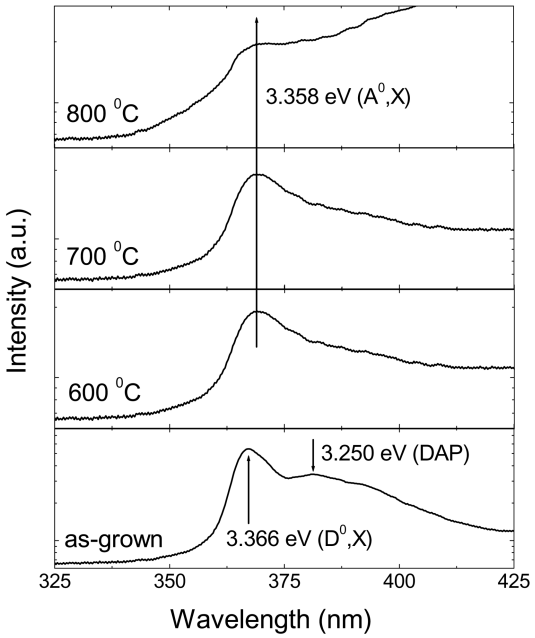

Fig. 5. The 15-K PL spectra taken from the as-grown and the ZnO:$P_{0.03}$ films annealed at 600, 700, and 800 °C. Note that, after RTA, the ZnO:$P_{0.03}$ films reveal a peak associated with the A^0,X emission.

3.2. P doping in ZnO using Zn_3P_2

The 3 mol% P-doped ZnO films (ZnO:$P_{0.03}$) were grown using the PLD. Their crystallinity and microstructure were basically the same as the As-doped ZnO films. The electrical properties of both the as-grown and annealed films were investigated by room temperature Hall effect measurements after being annealed in a flowing O_2 ambient for 3 min at various temperatures[22]. Figure 4 shows the variation in carrier concentration of the ZnO:$P_{0.03}$ films as a function of RTA temperature. The inset of Fig. 4 shows the variation in carrier concentration of the undoped and the ZnO:$P_{0.03}$ films, depending on the RTA temperature. Without annealing, the ZnO:$P_{0.03}$ films show somewhat higher carrier (electron) concentrations than the concentration of the undoped film, meaning that the incorporation of P renders them more conductive. As shown in Fig. 4, at RTA temperatures below 500 °C, the carrier concentrations slightly reduce; however, the ZnO:$P_{0.03}$ films exhibit a substantial reduction in their carrier concentration between 600 and 800 °C, implying that the activated P generates holes, sufficiently compensating electrons, and thereby reducing their electron concentration. But, for a further RTA temperature above 800 °C, the carrier concentration of the ZnO:$P_{0.03}$ films again increases. Although the ZnO:$P_{0.03}$ films annealed at RTA temperatures up to 500 °C and also above 800 °C show *n*-type conductivity, they exhibit a conversion of *p*-type from *n*-type conductivity in RTA temperatures ranging between 600 to 800 °C. The hole concentration, the mobility and the resistivity of the *p*-type ZnO:$P_{0.03}$ films are 5.1×10^{14}–1.5×10^{17} cm^{-3}, 2.38-39.3 cm^2/V-s, and 17-330 Ω-cm, respectively.

The PL spectra of ZnO:$P_{0.03}$ films annealed at higher RTA temperatures revealed pronounced defect-related emissions, data not shown, meaning that they contain a larger number of defects. We suppose that these defects highly compensate the hole carriers. The 15-K PL spectra of the as-grown ZnO:$P_{0.03}$ film and the films annealed at 600, 700, and 800°C are shown in Fig. 5. In the case of the as-grown film, the peaks observed at 3.366 eV, 3.378 eV, and 3.250 eV are, respectively, associated with the donor-bound exciton (D^0,X) emission[5], the A free-exciton (E_x,A) emission, and the emission due to the donor-acceptor pair (*DAP*) transition[35]. The PL spectra of the ZnO:$P_{0.03}$ films annealed between 300 and 500 °C as well as above 800°C, data not shown, revealed the peaks corresponding to the E_x,A and the D^0,X emissions. Interestingly, the ZnO:$P_{0.03}$ films annealed between 600 and 800°C, exhibit an emission at 3.358 eV, which can be ascribed to the A^0,X emission[17,27,28,29]. It may be noted that, being consistent with the Hall effect measurements, the A^0,X emission is observed only for the ZnO:$P_{0.03}$ films that show *p*-type conductivity.

XANES experiments were also conducted for the *n*-, and *p*-type ZnO:$P_{0.03}$ films. Figure 6 shows the O *K*-edge XANES spectra of both the *n*-type (as-grown) and the p-type (annealed) ZnO:$P_{0.03}$ films along with the spectrum obtained from the undoped ZnO bulk (reference sample). The XANES spectral features of the reference sample are in good agreement with the earlier reports, and also similar to the other TM oxides[36]. In the case of the *n*-type ZnO:$P_{0.03}$ film, the spectral features are assigned to O 2*p* – P 4*sp* hybridized states (A_2) and to O 2*p* – Zn 4*sp* states (B_2), respectively. In contrast, for the p-type ZnO:$P_{0.03}$ film, the features A_2 and B_2

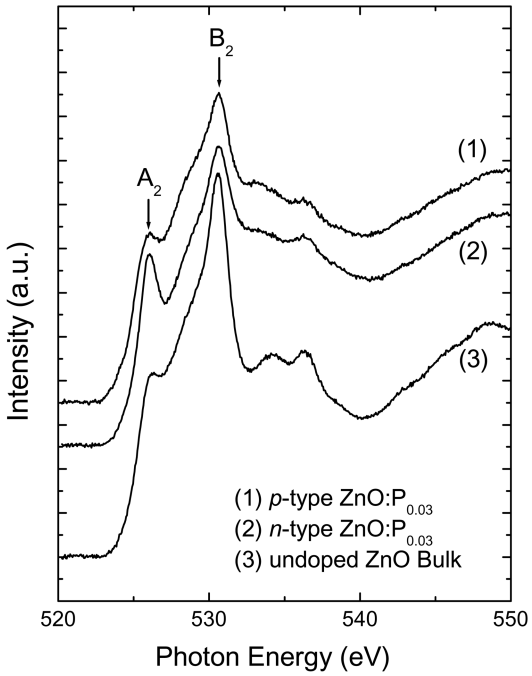

Fig. 6. The O *K*-edge XANES spectra of (1) *p*-type ZnO:$P_{0.03}$ film, (2) *n*-type ZnO:$P_{0.03}$ film, and (3) undoped ZnO bulk (reference sample). The XANES results indicates that P_O is the acceptor in the P-doped *p*-type ZnO films.

represent, respectively, O *2p* states and O 2*p* - Zn 4*sp* states. In comparing the undoped ZnO bulk with the *n*-type ZnO:$P_{0.03}$ film, the striking difference is that the latter reveals a high intense feature A_2 and a low intense feature B_2, meaning that the density of unoccupied states is significantly high in the as-grown state and the conduction is primarily due to the O *2p* - P 4*sp* hybridized states, which is consistent with the electrical properties of the same film. In contrast, after RTA, the intensity of the feature A_2 significantly decreases, whereas the feature B_2 increases. This indicates that the feature A_2 has no contribution from the P 4*sp* states after the process of thermal annealing, and thus it corresponds only to the holes at the O sites, indicating P substitutes for O sites, producing P_O, which is the acceptor in the P-doped *p*-type ZnO films. Detailed XANES measurements are in progress and the results will be published at a later date.

4. CONCLUSION

We deposited As-, and P-doped *p*-type ZnO films using Zn_3As_2/ZnO and Zn_3P_2/ZnO targets by using the PLD technique. Our experimental results suggest that both the Zn_3As_2 and Zn_3P_2 are promising *p*-type source materials for preparing reliable *p*-type ZnO. Results based on the x-ray absorption near-edge structure measurements provide useful information regarding the acceptors that are responsible for *p*-type behavior in the As-, and P-doped *p*-type ZnO films.

ACKNOWLEDGEMENTS

The authors are grateful for the financial support of the National Research Laboratory Program, funded by the Ministry of Science and Technology in Korea.

REFERENCES

1. D. C. Look, *Mater. Sci. Eng. B* **80**, 383 (2001).
2. U. Ozgür, Y. I. Alivov, C. Liu, A. Teke, M. A. Reshchikov, S. Doğan, V. Avrutin, S.J. Cho, and H. Morkoç, *J. Appl. Phys.* **98**, 041301 (2005).
3. S. F. Yu, C. Yuen, S. P. Lau, W. I. Park, and G. C. Yi, *Appl. Phys. Lett.* **84**, 3241 (2004).
4. K. Hara, T. Horiguchi, T. Kinoshita, K. Sayama, H. Sugihara, and H. Arakawa, Sol. Energy Mater. *Sol. Cells*. **64**, 115 (2000).
5. J. A. Rodriguez, T. Jirsak, J. Dvorak, S. Sambasivan, D. Fischer, *J. Phys. Chem. B* **104**, 319 (2000).
6. B. S. Panwar, *Appl. Phys. Lett.* **80**, 1832 (2002).
7. C. G. Van de Walle, *Phys. Rev. Lett*. **85**, 1012 (2000).
8. K. Minegishi, Y. Koiwai, and K. Kikuchi, *Jpn. J. Appl. Phys*., Part 2 **36**, L1453 (1997).
9. M. Joseph, H. Tabata, H. Saeki, K. Ueda, and T. Kawai, *Physica B* **302-303**, 140 (2001).
10. D. C. Look, D. C. Reynolds, C. W. Litton, R. L. Jones, D. B. Eason, and G. Cantwell, *Appl. Phys. Lett*. **81**, 1830 (2002).
11. X. Li, Y. Yan, T. A. Gessert, C. L. Perkins, D. Young, C. DeHart, M. Young, and T. J. Coutts, *J. Vac. Sci. Technol. A* **21**, 1342 (2003).
12. B. S. Li, Y. C. Liu, Z. Z. Zhi, D. Z. Shen, Y. M. Lu, J. Y. Zhang, X. W. Fan, R. X. Mu, and D. O. Henderson, *J. Mater. Res*. **18**, 8 (2003).
13. A. Zeuner, H. Alves, J. Sann, W. Kriegseis, C. Neumann, D. M. Hofmann, B. K. Meyer, A. Hoffmann, U. Haboeck, M. Straßburg, and A. Kaschner, *phys. stat. solidi. C* **1**, 731 (2004).
14. J. M. Bian, X. M. Li, C. Y. Zhang, W. D. Yu, and X. D. Gao, *Appl. Phys. Lett.* **85**, 4070 (2004).
15. C. C. Lin, S. Y. Chen, S. Y. Cheng, and H. Y. Lee, *Appl. Phys. Lett.* **84**, 5040 (2004).
16. A. Tsukazaki, A. Ohtomo, T. Onuma, M. Ohtani, T. Makino, M. Sumiya, K. Ohtani, S. F. Chichibu, S. Fuke, Y. Segawa, H. Ohno, H. Koinuma, and M. Kawasaki, *Nature Mater.* **4**, 42 (2005).
17. K.-K. Kim, H.-S. Kim, D.-K. Hwang, J.-H. Lim, and S.-J. Park, *Appl. Phys. Lett*. **83**, 63 (2003).
18. Y. W. Heo, S. J. Park, K. Ip, S. J. Pearton, and D. P. Norton, *Appl. Phys. Lett*. **83**, 1128 (2003).
19. W. Lee, D.-K. Hwang, M.-C. Jeong, M. K. Lee, M.-S. Oh, W.-K. Choi, and J.-M. Myoung, *Appl. Sur. Sci.* **221**, 32 (2004).
20. K. Ip, Y. W. Heo, D. P. Norton, S. J. Pearton, J. R.

LaRoche, and F. Ren, *Appl. Phys. Lett*. **85**, 1169 (2004).
21. Z. G. Yu, H. Gong, and P. Wu, *Chem. Mater.* **17**, 852 (2005).
22. V. Vaithianathan, B-T, Lee, and S. S. Kim, *J. Appl. Phys*. **98**, 043519 (2005).
23. Y. R. Ryu, W. J. Kim, and H. W. White, J. Cryst. Growth **219**, 419 (2000).
24. Y. D. Ko, J. Jung, K. H. Bang, M. C. Park, K. S. Huh, J. M. Myoung, and L.Yun, *Appl. Sur. Sci*. **202**, 266 (2002).
25. J. F. Rommeluere, L. Svob, F. Jomard, J. M. Arroyo, A. Lusson, V. Sallet, and Y. Marfaing, *Appl. Phys. Lett*. **83**, 287 (2003).
26. Y. R. Ryu, T. S. Lee, and H. W. White, Appl. Phys. Lett. 83, 87 (2003).
27. D. C. Look, G. M. Renlund, R. H. Burgener II, and J. R. Sizelove, *Appl. Phys. Lett.* **85**, 5269 (2004).
28. T. S. Jeong, M. S. Han, C. J. Youn, and Y. S. Park, *J. Appl. Phys*. **96**, 175 (2004).
29. V. Vaithianathan, B-T, Lee, S. S. Kim, *Appl. Phys. Lett*. **86**, 062101 (2005).
30. T. Aoki, Y. Shimizu, A. Miyake, A. Nakamura, Y. Nakanishi, and Y. Hatanaka, *phys. stat. sol.* (*b*) **229**, 911 (2002).
31. P. Fons, K. Nakahara, A. Yamada, K. Iwata, K. Matsubara, H. Takasu, and S. Niki, *phys. stat. sol*. (*b*) **229**, 849 (2002).
32. T. Yamamoto and H. Katayama-Yoshida, *Jpn. J. Appl. Phys*. **38**, L166 (1999).
33. Sukit Limpijumnong, S. B. Zhang, Su-Huai Wei, and C. H. *Park, Phys. Rev. Lett.* **92**, 15155504-1 (2004).
34. J. Stohr, *NEXAFS Spectroscopy*, Springer, Berlin, (1992).
35. B. K. Meyer, H. Alves, D. M. Hofmann, W. Kriegseis, D. Forster, F. Bertram, J. Christen, A. Hoffmann, M. Straβburg, M. Dworzak, U. Haboeck, and A. V. Rodina., *phys. stat. sol*. (*b*) **241**, 231 (2004).
36. J. G. Chen, B. Fruhberger, and M. L. Colaianni, *J. Vac. Sci. Technol. A* **14**, 1668 (1996).